Shape Analysis and Fuzzy Control for 3D Competitive Segmentation of Brain Structures with Level Sets

Cybèle Ciofolo and Christian Barillot

IRISA / CNRS, Team VisAGeS,
Campus de Beaulieu, 35042 Rennes Cedex, France
{Cybele.Ciofolo, Christian.Barillot}@irisa.fr
http://www.www.irisa.fr/visages/visages-eng.html

Abstract. We propose a new method to segment 3D structures with competitive level sets driven by a shape model and fuzzy control. To this end, several contours evolve simultaneously toward previously defined targets. The main contribution of this paper is the original introduction of prior information provided by a shape model, which is used as an anatomical atlas, into a fuzzy decision system. The shape information is combined with the intensity distribution of the image and the relative position of the contours. This combination automatically determines the directional term of the evolution equation of each level set. This leads to a local expansion or contraction of the contours, in order to match the borders of their respective targets. The shape model is produced with a principal component analysis, and the resulting mean shape and variations are used to estimate the target location and the fuzzy states corresponding to the distance between the current contour and the target. By combining shape analysis and fuzzy control, we take advantage of both approaches to improve the level set segmentation process with prior information. Experiments are shown for the 3D segmentation of deep brain structures from MRI and a quantitative evaluation is performed on a 18 volumes dataset.

1 Introduction

During the last decade, segmentation methods have become more and more sophisticated, in order to deal with very complex problems, such as texture segmentation, motion detection or medical imaging segmentation. Some approaches have now proved to be adapted to certain type of applications. In particular, the level set methods first proposed by Osher and Sethian [1] have become very common in the computer vision community and are now used in various contexts. The reason for such a broad field of applications is their implicit, intrisic, parameter and topology free formulation. In particular, they provide a very efficient framework for 3D image segmentation, where many 2D methods are difficult to apply.

A. Leonardis, H. Bischof, and A. Pinz (Eds.): ECCV 2006, Part I, LNCS 3951, pp. 458–470, 2006.

After the first contour-based algorithms [2, 3], more sophisticated methods have been proposed, using regional statistics [4] or both contour and region terms [5] to segment 3D structures, moving objects [6] or textured content of images [7]. But both contour and region constraints are generally derived from the grey levels of the image, and do not always provide enough information to segment complex structures with variable shapes, particularly if their borders do not appear clearly in the images, as it often occurs in medical imagery for example. For this reason, prior information in general and shape models [8] in particular have been widely associated with level sets for image segmentation.

For example, Rousson and Paragios propose an elegant introduction of shape priors in a variational framework to perform a level-set based segmentation of noisy or occluded data [9]. Tsai *et. al.* also take advantage of a shape model obtained by training to drive the evolution of a 3D contour [10], and Yang *et. al.* introduce a joint intensity-shape prior in a probalistic segmentation with level sets [11].

It sometimes happens however that the segmentation targets have very blurred borders, and that the grey levels inside these structures are not really homogeneous and even similar to that of neighboring objects. This phenomenon occurs for example in the deep grey structures of the brain, which may be difficult to distinguish from white matter. In this context, even shape information is sometimes not sufficient to achieve an accurate segmentation. A very useful framework is however provided by the fuzzy set theory, which is adapted to model non-precise knowledge, as, for instance, objects with ill-defined borders.

Consequently, the fuzzy sets theory has already been used in image segmentation, especially in medical imaging. Xu *et. al* use an adaptative fuzzy c-means algorithm that is combined with an isosurface algorithm and a deformable surface model to reconstruct the brain cortex [12]. Automatic segmentation methods for brain internal structures are also proposed [13], where the segmentation is based on a symbolic spatial description of the structures and finally refined with a deformable model.

In this article, our goal is to present a methodology which takes advantage of three approaches that have proved to give good results in different contexts: level set segmentation, shape modeling and fuzzy logic. The objective is to be able to segment several objects which borders do not appear clearly, and which can not be distinguished with only image statistics. As this is a very complex problem, which however occurs very often in medical imagery, the use of a single segmentation method would lead to a very complex mathematical modeling and difficult implementation. To avoid this, we combine a basic shape model and a very simple type of fuzzy decision system to locally drive the evolution of several level sets, which are simultaneously deformed to reach their respective targets. In previous work [14], we presented a preliminary version of this methodology which did not include any shape model, and applied it to the segmentation of brain structures. In this paper, we show how the use of a preliminary shape analysis strongly improves the robustness of the method. The algorithm is applied on

a real Magnetic Resonance Images (MRI) dataset, in order to segment internal brain structures, which are of great interest for the quantitative morphological analysis of neurological pathologies.

This paper is organized as follows: Section 2 summarizes the principle of our level set segmentation driven with fuzzy control, Section 3 presents the construction of the shape model and experimental results are shown and discussed in Section 4. Finally, we conclude in Section 5.

2 Level Set Segmentation Driven by Fuzzy Control

In this section we briefly present how a fuzzy decision system tunes the terms of the evolution equations of several level sets. More details about this method can be found in [14].

2.1 General Principle

As we wish to segment simultaneously several structures in the same volume, we assign one level set (represented by one contour) to each target. As the level set formalism allows topological changes, a single target may be composed of several components, and the corresponding contour can split or merge. We use the level set equation evolution proposed in [15]:

$$F = g(P_T)(\rho\kappa - \nu), \tag{1}$$

where ν is a constant module force, whose sign leads the current contour toward the desired border; κ is the local curvature of the contour; ρ is the weight on curvature; g is a decreasing function; and P_T is the probability of transition between the inside and the outside of the structure to be segmented. Thus the role of the term $g(P_T)$ is to stop the evolution of the contour at the desired location.

The ν and P_T terms are computed according to a preliminary classification of tissues before the beginning of the level set evolution. The image intensities are viewed as samples of a Gaussian Mixture Model (GMM), whose parameters are estimated according to a Maximum A Posteriori principle, with a SEM algorithm [16]. The classes that are mainly represented inside the initialisation volume are automatically detected and determine the reduced GMM corresponding to the inside of the object to segment. For further details concerning the computation of these terms, see [15].

The advantages of the evolution force described in Eq. (1) is that it is very simple and directly derived from the original geometric active contour formulation [3]. It assigns a precise role to each term, while preserving the ability to modify each term according to geometrical constraints corresponding to visual requirements.

2.2 Non-overlapping Constraint

Each target has a physical meaning, which implies that they should not overlap. Consequently, the deformation of the contours needs to respect this non-

overlapping constraint. This is generally done by using additional terms corresponding to an external force in the equation evolution of the level sets.

Recent approaches [4, 5] generally use energy minimization techniques to define the additional terms of the force. However, in medical imaging, the structures of interest are often very small compared to the image resolution and may have complex shapes. This makes it difficult to define energy constraints that remain both general and adapted to specific structures and pathologies. Another approach consists in translating the available information into decision rules that are directly used to drive the level set evolution. This can be done with the fuzzy set theory, which is very convenient to express rules in natural language.

We designed our method considering two main objectives: the implementation should be as simple as possible, and all the information provided by the data should be exploited. This lead us to use a particular type of fuzzy decision system: a fuzzy controller, both for its simplicity and ability to deal with precise measurements. The role of this fuzzy controller is to drive the different contours to their respective targets, while avoiding overlapping. This is directly related to Eq. (1), where the ν term determines the privileged evolution direction of the contour. Consequently, the output of the fuzzy controller is ν, and is calculated for each voxel, at each iteration of the evolution.

2.3 Fuzzy Controller

In [15], the proposed formulation for ν is given by:

$$\nu = \text{Sign}(P(\lambda \in \Lambda_i|\mathbf{x}) - P(\lambda \in \Lambda_e|\mathbf{x})), \tag{2}$$

where $\mathbf{x}$ is the current voxel, λ is the class of the current voxel estimated from the volume histogram, and Λ_i and Λ_e are the reduced GMM representing respectively the inside and the outside of the structure to be segmented. As this equation doen not take into account the notion of segmentation target nor any non-overlapping constraint, the fuzzy controller replaces it by the following constraints:

1. Several contours that evolve in competition must not intersect even if each of them can split in several components;
2. Each contour must stay in the vicinity of the fuzzy label describing its segmentation target;
3. Eq. (2) is valid under Conditions 1 and 2.

Condition 1 is the non-overlapping constraint and may be related to some other methods, such as multiphase level sets [4]. However this approach is applicable if the regions can be distinguished by their statistics. In the case of regions presenting similar grey levels, such as the brain grey nuclei, one must use other features, like labels coming from an atlas, to guarantee that the different contours will not intersect. Another approach consists in using a repulsive evolution force [17, 7, 18]. Our method is similar to these ones, since the ν term defines a locally adaptive force. However, the advantage of the fuzzy controller is that this force can be defined even if homogeneous regions do not appear clearly in the image.

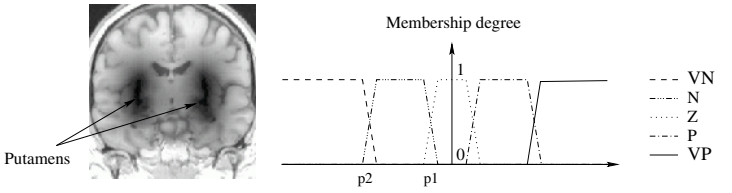

Fig. 1. Left: distance map from the putamens. Right: the five fuzzy states of *Dlab*: very negative (VN), negative (N), around zero (Z), positive (P) and very positive (VP).

Table 1. Fuzzy decision rules for the output variable ν. The states of *Dlab* are very negative (VN), negative (N), around zero (Z), positive (P), and very positive (VP). The states of the variable *Dc* are null (N), too close (TC), close (C), rather close (RC) and far (F). The states of the variables *Dp* and ν are negative (N) and positive (P).

	Dlab=VN		*Dlab*=N		*Dlab*=Z		*Dlab*=P		*Dlab*=VP	
	Dp=N	*Dp*=P	*Dp*=N	*Dp*=P	*Dp*=N	*Dp*=P	*Dp*=N	*Dp*=P	*Dp* =N	*Dp*=P
Dc=N	N	N	N	N	N	N	N	N	N	N
Dc=TC	N	N	N	N	N	P	N	P	P	P
Dc=C	N	N	N	N	N	P	N	P	P	P
Dc=RC	N	N	N	N	N	P	N	P	P	P
Dc=F	N	N	N	N	N	P	N	P	P	P

In order to take the three conditions listed above into account, we define three fuzzy variables as inputs of the fuzzy controller:

1. *Dc* represents the distance from the current contour to the other ones.
2. *Dlab* represents the signed distance from the current contour to the label corresponding to its segmentation target. An example of distance map, or fuzzy label map of the brain putamens is shown on Fig. 1.
3. *Dp* represents the difference of probability presented in Eq. (2).

These variables are then combined to define the fuzzy decision rules determined by the three conditions. The five states of each input and the rules are summarized in Table 1. They are used to assign a *positive* or *negative* state to ν, which respectively mean that the contour will locally expand or contract. We use only two states to caracterize ν, since it has been shown that only its sign has a real influence on the contour evolution [15].

Condition 2, which is related to the distance maps, is translated by a majority of P states in the right part of the table and N states in the left part. This means that if the processed voxel of the contour is far outside its label (*Dlab*=N or VN), it needs to contract (ν=N). On the contrary, if it is inside the label (*Dlab*=P or VP), it needs to expand (ν=P).

Condition 3 is mainly visible in the central part of the table (*Dlab*=Z and *Dc*=TC to F). This corresponds to the case where the contour is within the

vicinity of its label and not too close to another one. Then the state of ν depends on the intensities of the volume only, as explained in Eq. (2).

This fuzzy controller is thus used to determine ν for each voxel, at each iteration of the segmentation process. Let us note that even if there are several contours, only one fuzzy controller is needed and used alternatively for each of them. Moreover, the expression of the propagation conditions in natural language avoids the use of weighting parameters in the evolution equation of the level sets, which is an advantage compared to many variational approaches. More details about the implementation are available in [14].

3 Shape Analysis for Level Set Segmentation

This part explains how a shape model is constructed and used to define the fuzzy variable *Dlab*, in order to be introduced in the segmentation process with level sets and fuzzy control.

3.1 Construction of the Shape Model

As many authors do, we use a principal component analysis (PCA) to construct the shape model. The main reason for this choice is that PCA provides the parameters of variation modes that are ordered according to their representativity. We thus take advantage of this property to define the fuzzy states of *Dlab*.

For each target, the PCA is performed on a population of n shapes that have previously been registered in the same referential as the processed volume and segmented. A shape is then represented by a vector $\mathbf{x_i}, i \in \{1, \ldots, n\}$, which components are the grey levels of the volume containing the shape. The mean shape $\bar{\mathbf{x}}$ is given by $\bar{\mathbf{x}} = \frac{1}{n} \sum_{i=1}^{n} \mathbf{x}_i$. The covariance matrix of the shape population is diagonalized in order to provide n eigenvalues $\lambda_1 \geq \cdots \geq \lambda_n$ and the associated eigenvectors, which constitute the matrix $\mathbf{\Phi}$. The variation modes represented by $\mathbf{\Phi}$ are ordered according to their respective eigenvalues. New samples $\tilde{\mathbf{x}}$ corresponding to the model can then be generated by using:

$$\tilde{\mathbf{x}} = \bar{\mathbf{x}} + \mathbf{\Phi_m} \mathbf{b_m}, \tag{3}$$

where $\mathbf{\Phi_m}$ is a submatrix of $\mathbf{\Phi}$ representing m selected variation modes and $\mathbf{b_m}$ are the b_i weightings corresponding to each mode, $i \in \{1, \ldots, m\}$.

3.2 Introduction of the Shape Model in the Segmentation Process

Using a shape model to drive a segmentation method has become very common since the introduction of Active Shape Models [8]. However, these models strongly depend on the parametrisation of the shapes, which makes it difficult to use them in 3D. As we would like to avoid this dependance, we use a level set formalism instead of a parametric deformable model, as in [11, 10].

The shape model obtained by PCA is used for two purposes: (1) defining the segmentation target labels and (2) estimating the fuzzy states of the variable *Dlab*, which represents the distance to these labels. These two steps are now described for a given target.

Definition of the segmentation target label
A fuzzy label is used to approximately locate the target in the volume. It is created by applying a distance transformation [19] on the mean shape obtained by PCA.

Definition of the fuzzy states of *Dlab*
We assume that there is a relationship between the variation modes of the shape obtained by PCA and the area that is actually covered by the real target on the image. Indeed, let us consider the largest variation allowed by the shape model, by selecting large values of b_i in Eq. (3). They are likely to correspond to shapes which are very different from the mean shape, but remain realistic. Thus, the distance between these generated shapes and the label defined by the mean shape can be viewed as an indicator of which distance can be considered as *very negative* for *Dlab*.

We proceed as follows. First an appropriate number m of modes is selected in order to be able to generate shapes that correctly represent the variability of the structure. This is done by choosing m so that the cumulated variances of the first m modes are greater than 66% of the total variance. This is possible due to the ordering of modes provided by PCA.

Then we consider that small shape variations correspond to $|b_i| \leq \sqrt{\lambda_i}$ and large variations correspond to $|b_i| \leq 3\sqrt{\lambda_i}$, since $P(|b_i| \leq \sqrt{\lambda_i}) = 68\%$ and $P(|b_i| \leq 3\sqrt{\lambda_i}) = 99,7\%$. The corresponding "small variation" and "large variation" shapes are generated. An example is shown on Fig. 2.

Fig. 2. Areas covered by variations around the mean shape for both putamens. Dark grey: mean shape, light grey: small var. ($|b_i| = \sqrt{\lambda_i}$), white: large var. ($|b_i| = 3\sqrt{\lambda_i}$).

Finally, the mean distance between the mean shape and the "small variation" shape defines the point p_1 on Fig. 1, which distinguishes the *negative* and *around zero* states of *Dlab*. The mean distance between the mean shape and the "large variation" shape defines the point p_2 on Fig. 1, which is located between the *very negative* and *negative* states of *Dlab*. The points corresponding to the limits between the states *around zero*, *positive* and *very positive* are obtained by symmetry with respect to zero.

As there are several segmentation targets, this process is repeated for each of them, and we finally take the average p_1 and p_2 values to define *Dlab*. This averaging operation may be considered as information loss, since *Dlab* is not specific to each target. However, in practice, the structures to be segmented have approximately the same size, and their p_1 (respectively p_2) values are similar,

which allows us to average them. The advantage of this approach is that we define a single fuzzy controller for all the targets, and thus reduce computation time and memory needs.

The main advantage of this method is that the fuzzy states of *Dlab* are determined by the statistical analysis, instead of being estimated arbitrarily by an expert. This is a step forward in reducing the number of manually tuned parameters of the segmentation algorithm.

4 Application: Internal Brain Structures Segmentation

The method is applied to segment the brain grey nuclei, which are internal brain structures located in the deep grey matter. We focus on four segmentation targets: (1) left and right thalamus, (2) left and right caudate nucleus, (3) left and right pallidum and (4) left and right putamen. Each target is thus made of two parts, and we use four level sets for the segmentation, one for each target.

The grey nuclei are very difficult to segment, since their grey levels are not homogeneous and their borders with the surrounding white matter do not appear clearly on MRI. Consequently, even when they are segmented manually by experts, the results vary a lot according to the level of experience and the attention of the human observer. From a medical point of view, these structures are strongly involved in many neurological pathologies, which means that an automated segmentation method is critical to perform morphomotric analyses on large populations, without suffering from the variability of manual results. The grey nuclei are also a target for electro-stimulation in the treatment of Parkinson's disease. The segmentation is thus very useful to plan the surgical intervention.

4.1 Data

We test our method on a database provided on the Internet Brain Segmentation Repository (IBSR), and available at the Center for Morphometric Analysis, Massachusetts General Hospital (`http://www.cma.mgh.harvard.edu/ibsr`).

This database contains 18 real T1-weighted MR scans and the corresponding manual segmentation of 43 structures, performed by a trained expert. We consider this manual segmentation as the ground truth to assess our results. The MR scans are $256 \times 256 \times 128$ volumes, with slices of thickness 1.5mm, and pixel dimension going from 0.84mm to 1mm on each slice.

4.2 Experiments

In order to show the improvement brought by shape analysis, we present three different experiments:

- Exp. 1: segmentation of the grey nuclei without shape analysis,
- Exp. 2: segmentation of the grey nuclei with shape analysis for the propagation of the level sets (with the same initialisation as Exp. 1),
- Exp. 3: segmentation of the grey nuclei with shape analysis for the propagation and the initialisation of the level sets.

The first two experiments show the role of the shape analysis in the same conditions, and the third one demonstrates how the results can be improved by adding more prior information in the segmentation process.

Choice of the atlas and labels
For all experiments, an atlas is needed to define the fuzzy labels corresponding to the segmentation targets. For Exp. 1 (without shape analysis), one subject of the dataset is randomly chosen to be the atlas, and the segmentation is performed on the 17 other subjects. The fuzzy labels of the targets are then obtained from the manual segmentation associated to the atlas with a linear registration algorithm (12 parameters that maximise the mutual information are computed). As the manual results are subject to intra and inter-observer variability, it is likely that these labels are not accurate enough to drive the propagation of the contours properly. This motivates the use of a statistical analysis to construct a shape model which is used as an atlas. Consequently, for Exp. 2 and 3, a leave-one-out process is applied to construct the shape model of the targets as explained in Section 3. The statistical analysis is done from the manual segmentation associated with every subject but the processed one. To this end, the registration between the shapes is done with the same registration algorithm with 12 parameters. We select 5 modes, since this corresponds to a cumulated variance greater than 66% of the total variance, but in practice, we observe that the results are approximately the same for 3 modes or more.

Initialisation and results
For Exp. 1, the contours are initialised by doing a morphological erosion on the target labels. For Exp. 2, we use exactly the same initialisation to be able to compare the results with and without shape analysis. We also tried to use boxes roughly located in the center of the brain as initialisation. This lead to quite good results, but the computation time was larger and even if the final locations of the contours was satisfying, there were some inaccuracies along the borders, where the initialisation was not consistent with the location of the targets.

For Exp. 3, we include more prior information in the segmentation process, by using a better initialisation. This is done by performing a morphological erosion on the labels obtained by shape analysis, instead of the labels obtained by registration from one subject.

Let us stress that for comparison purposes, all the tests are run with the same set of parameters for all experiments and all subjects.

The segmentation takes approximately 15 to 20 minutes on a 3GHz Linux PC with 1GB memory. The results are good for 15 subjects. The registration does not perform very well for the 2 remaining subjects, and even if the segmentation process tempts to counteract this effect, the results are not accurate enough, which means that even if the global location is good, the borders of the target are not properly recovered. An example of results is shown on Fig. 3.

These results show that without shape analysis (top row), the grey nuclei, especially the putamens and pallida are over-segmented, while the global shape of the thalami is not completely realistic. This is corrected by the shape analysis, on

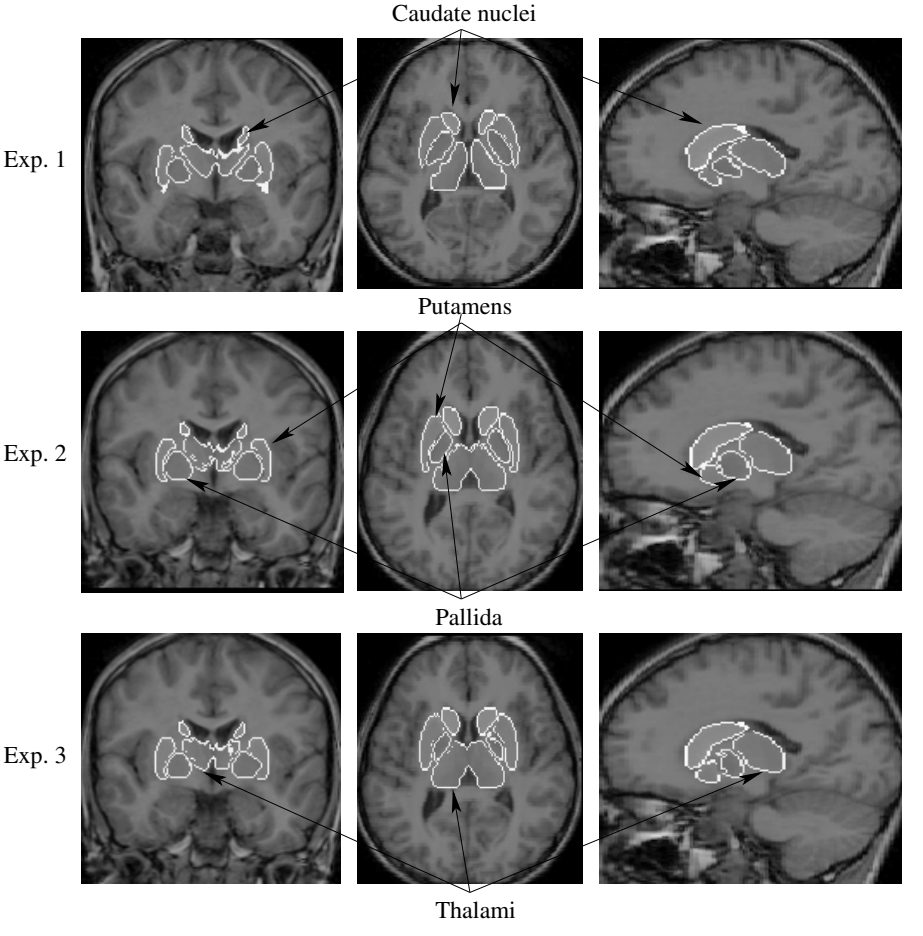

Fig. 3. Segmentation of the grey nuclei. Top row: without shape analysis, middle row: with shape analysis for the propagation of the level sets only, bottom row: with shape analysis for the propagation and the initialisation of the level sets.

the middle and bottom rows. Moreover, the segmentations shown on the middle and bottom rows look rather the same, which means that even if the initialisation used in Exp. 3 improves the results, this is an additional improvement that does not have as much influence as the use of the shape model to drive the propagation of the contours.

4.3 Quantitative Evaluation

In order to quantitatively assess our results on the IBSR dataset, we compute the mean distance M_d between our results and the ground truth provided by the manual segmentation. We also use the spatial accuracy index S, which is a similarity index based on the overlapping rate between the result and the truth [20]:

$$S = 2 \cdot \frac{\text{Card}(R \cap T)}{\text{Card}(R)+\text{Card}(T)} \quad M_d = \frac{\sum_{r \in R} \min_{t \in T} d(r,t)}{\text{Card}(R)},$$

where R is the segmentation result and T is the ground truth. Our results are summarized in Table 2. This table also contains the S and M_d values corresponding to the similarity between the 12-parameter registration result of the atlas structures and the ground truth.

Table 2. Similarity indice S and mean distance M_d for the segmentation of the thalami (Th.), caudate nuclei (CN), pallida (GP) and putamens (Pu.), with or without shape analysis (S.A.)

	Th.		NC		GP		Pu.	
	S	M_d	S	M_d	S	M_d	S	M_d
Registration	0.73	1.8	0.60	1.9	0.53	2.1	0.66	1.8
Exp. 1: Without shape analysis	0.77	1.7	0.60	2.1	0.56	2.0	0.62	1.9
Exp. 2: With S.A. for propagation	0.82	1.5	0.64	2.2	0.67	1.7	0.68	1.8
Exp. 3: With S.A. for prop. and init.	0.82	1.5	0.64	2.1	0.62	1.8	0.74	1.5

The table clearly shows that the segmentation results, especially with shape analysis, are better than the registration ones. The spatial accuracy index is good for the thalami. For the caudate nuclei, pallida and putamens, the lower values can be explained by the small size of the corresponding structures. Consequently, even a small difference between the result and the ground truth leads to a large variation in the spatial accuracy index. As an example, let us consider the result of a morphological erosion on the ground truth of one of these structures with a structuring element of size 1. The mean S value computed between the ground truth and the erosion result is only 0.77. This is the reason why, in literature, an S value greater than 0.7 is considered as a very good result [20]. Moreover, it is well-known that a manual segmentation performed by only one expert is not enough to be a real gold standard. An offset of one or two voxels with respect to the ground truth we use is thus acceptable.

Finally, the M_d values are low for all the grey nuclei, even the small ones which do not have very good S values. They are also significantly decreased by the use of the shape analysis for the propagation of the contours, and even more if the shape analysis is used for initialisation. As the quantitative results include the 2 cases on which the registration fails, these low M_d values show that the segmentation is more effective than registration only, and strongly improved by shape analysis. This is also demonstrated by the standard deviation of the mean M_d values, which is largely lower for segmentation with shape analysis (less than 0.3 voxels except for caudate nuclei) than for registration (around 0.5 voxels).

Moreover, as the segmentation parameters were the same for all the subjects in the dataset, it is obvious that these results are not optimal for each subject, but show the robustness of the method when used on several different volumes.

5 Conclusion and Future Work

We proposed a level set segmentation method which originally combines a statistical shape analysis and a fuzzy controller. Shape analysis and fuzzy control bring prior information in the segmentation process, while keeping the implementation of the method simple, which allows us to segment several structures simultaneously. The quantitative assessment of the experimental results show that the segmentation of small and blurred structures is strongly improved by shape analysis, and more accurate than registration.

Future work concerns the adaptation and application of the method to other small objects, using other types of prior information. In particular, the brain hippocampi and amygdala are particularly interesting to segment for medical purposes. This is a very difficult task since they are very small and their shape is highly variable, which makes their automated segmentation a challenge.

Acknowledgements

We thank the Center for Morphometric Analysis at Massachusetts General Hospital (`http://www.cma.mgh.harvard.edu/ibsr/`) for providing the MR brain data sets and their manual segmentations.

This work was supported by the CNRS and the Region Bretagne Council.

References

1. Osher, S., Sethian, J.A.: Fronts propagating with curvature dependant speed: algorithms based on Hamilton-Jacobi formulation. Jour. Comp. Phys. **79** (1988) 12–49
2. Caselles, V., Kimmel, R., Sapiro, G.: Geodesic active contours. Int. Jour. Comp. Vis. **22** (1997) 61–79
3. Malladi, R., Sethian, J.A., Vemuri, C.: Shape modeling with front propagation: a level set approach. IEEE Trans. Patt. Anal. Mach. Intell. **17** (1995) 158–175
4. Vese, L.A., Chan, T.F.: A multiphase level set framework for image segmentation using the Mumford and Shah model. Int. Jour. Comp. Vis. **50** (2002)
5. Paragios, N.: A variational approach for the segmentation of the left ventricle in cardiac image analysis. Int. Jour. Comp. Vis. **50** (2002) 345–362
6. Paragios, N., Deriche, R.: Geodesic active contours and level sets for the detection and tracking of moving objects. IEEE Trans. Patt. Anal. Mach. Intell. **22** (2000) 266–280
7. Paragios, N., Deriche, R.: Coupled geodesic active regions for image segmentation: a level set approach. In: Eur. Conf. Comp. Vis. (ECCV). (2000) 224–240
8. Cootes, T.F., Taylor, C.J., Cooper, D.H., Graham, J.: Active shape models - their training and application. Comp. Vis. Im. Underst. **61** (1995) 38–59
9. Rousson, M., Paragios, N.: Shape priors for level set representations. In: Eur. Conf. Comp. Vis. (ECCV). (2002) 78–92
10. Tsai, A., et. al.: A shape-based approach to the segmentation of medical imagery using level sets. IEEE Trans. Med. Imag. **22** (2003) 137–154

11. Yang, J., Duncan, J.S.: 3D image segmentation of deformable objects with joint shape-intensity prior models using level sets. Med. Image Anal. **8** (2004) 285–294
12. Xu, D.L., et. al.: Reconstruction of the human cerebral cortex from magnetic resonance images. IEEE Trans. Med. Imag. **18** (1999) 467–480
13. Colliot, O., Camara, O., Dewynter, R., Bloch, I.: Description of brain internal structures by means of spatial relations for MR image segmentation. In: Int. Soc. Opt. Eng. SPIE Med. Imag. (2004) 444–455
14. Ciofolo, C., Barillot, C.: Brain segmentation with competitive level sets and fuzzy control. In: Int. Conf. Inform. Proc. Med. Imag.(IPMI). (2005) 333–344
15. Baillard, C., Hellier, P., Barillot, C.: Segmentation of brain 3D MR images using level sets and dense registration. Med. Image Anal. **5** (2001) 185–194
16. Celeux, G., et. al.: L'algorithme SEM : un algorithme d'apprentissage probabiliste pour la reconnaissance de mélanges de densités. Rev. Stat. App. **34** (1986) 35–51
17. Zhao, H.K., Chan, T., Merriman, B., Osher, S.: A variational level set approach to multiphase motion. Jour. Comp. Phys. **127** (1996) 179–195
18. Samson, C., Blanc-Féraud, L., G., A., Zerubia, J.: A level set model for image classification. Int. Jour. Comp. Vis. **40** (2000) 187–197
19. Borgefors, G.: Distance transformations in digital images. Comp. Vis. Graph. Im. Proc. **34** (1986) 344–371
20. Zijdenbos, A.P., Dawant, B.M., Margolin, R.A., Palmer, A.C.: Morphometric analysis of white matter lesions in MR images: method and validation. IEEE Trans. Med. Imag. **13** (1994) 716–724